Pure & Appl.Chem., Vol.53, pp.2083-2094.
Printed in Great Britain.

0033-4545/81/112083-12$02.00/0
Pergamon Press Ltd

COLLOID SPECTROSCOPY

Milton Kerker

Clarkson College of Technology, Potsdam, New York 13676, USA

Abstract - The ability of small particles to separate light spectrally has played a major role in optical studies of size dependent colloidal phenomena. In this lecture, surface enhanced Raman scattering (SERS) will be utilized as an illustration of colloid spectroscopy. SERS occurs for molecules adsorbed at the surface of colloidal particles as well as at roughened macroscopic surfaces. An advantage of working with colloidal systems is that the main features of SERS can be accounted for by a classical electrodynamic model which takes into account the size, shape and optical constants of the colloidal particles.

> ...and God said unto Noah, I do set my bow in the cloud and it shall be for a token of a covenant that the waters shall no more become a flood to destroy all flesh.
>
> Genesis, Chapter 9

1. INTRODUCTION

I have used the term colloid spectroscopy for the title of this talk in order to point out that scattering by small particles may serve to separate light spectrally. The blue of the sky, the russets of sunrise and sunset, the rainbow, stained glass and brilliantly colored metal hydrosols are among such light scattering phenomena that are both awesome and beautiful. More than a century ago Michael Faraday proposed that the colors exhibited by silver and gold hydrosols might be due to the various degrees of subdivision of the metal particles comprising these sols. He noted that

> ...gold is reduced in exceedingly fine particles, which becoming diffused, produce a beautiful ruby fluid... the various preparations of gold, whether ruby, green, violet or blue...consist of that substance in a metallic divided state.
>
> Michael Faraday, The Bakerian Lecture, Feb. 5, 1857. Phil. Trans. 147, 145 (1857).

This connection, between particle size and the optical properties of colloidal dispersions was resolved in 1908 by Gustav Mie in a paper which has laid the basis for subsequent work in colloid optics. Although earlier workers had already solved the general problem of light scattering by a sphere, Mie addressed himself specifically to the question of the origin of the color of metal hydrosols. The appearance of a bulk metal is determined by its reflectance and this depends in a direct way upon the variation of the complex refractive index with wavelength. The color of a colloidal dispersion is determined by the wavelength dependence of the scattered light intensity. This is not only a very complicated function of complex refractive index but also of particle size and shape. One of the results of Mie's theory is shown

in Fig. 1 where the scattering intensity calculated for spherical gold particles is plotted versus wavelength for irradiation by white light. It is apparent, as Mie notes, that as the particles become larger the color changes from yellow to red.

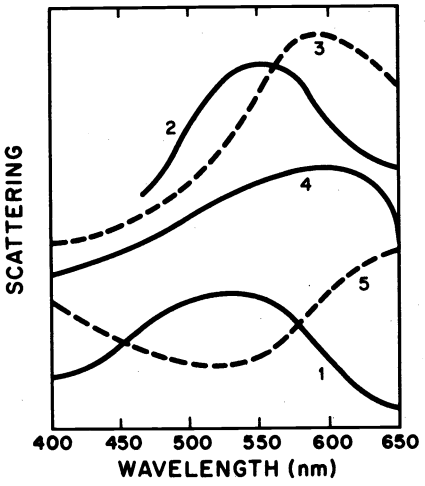

Fig. 1. Scattering cross section vs. wavelength for gold hydrosol. Diameters and colors: (1) 60 nm, yellow, (2) 100 nm, (3) 120 nm, (4) 140 nm, (5) 180 nm, red. "Je grösser sie werden, um so mehr verändert sich ihre farbe zu gelb zu rotgelbe," G. Mie, Ann. Physik 25, 377 (1908).

Mie's analysis and the theoretical developments which have followed, when combined with recent advances in both laboratory and computer technology, have opened up vast new possibilities for optical studies of size dependent colloidal phenomena and my initial plans for this talk were to illustrate various recent advances by examples both from our own work and from that of others. Alas, even a rough sketch hardly permits one to scratch the surface and so rather than survey a number of topics I have chosen finally to consider only a single phenomenon, surface enhanced Raman scattering, which is also known by the acronym SERS. This is a subject about which there is much current discussion and controversy. I will try to convince you that the phenomenon can be understood in terms of classical colloidal spectroscopy. That at least may justify the title of the talk. Indeed, we will see that the very same physical effects that give rise to the colors of silver and gold hydrosols investigated by Michael Faraday and Gustave Mie are also responsible for SERS.

Raman scattering has not been a part of the vast array of surface sensitive spectroscopic techniques developed in recent years, even though it offers great advantages for determining the identity of adsorbed chemical species. The problem has been that the intensity of normal Raman scattering from a monolayer adsorbed on a macroscopic surface is much too low for practical detection.

Fleischmann, Hendra and McQuillan, in England, in a series of papers starting in 1974 sought to overcome this limitation by working with pyridine adsorbed at a silver electrode surface which had been roughened by successive oxidation-reduction cycles. The main idea was that silver has a very high adsorptivity, that pyridine has a high Raman cross section, and that the increased surface area of the roughened surface would permit adsorption of a still larger number of molecules. Indeed, they obtained remarkably strong Raman signals but mistakenly attributed these to the increased surface concentration of pyridine at the roughened surface.

It was not until 1977 that Jeanmaire and Van Duyne in the US and Albrecht and Creighton in England demonstrated that the signals were enhanced by a factor roughly estimated to be from 10^5 to 10^6 over what would be expected from a monolayer and that such a remarkable result could in no way be explained by an increase in surface area. It was a new phenomenon.

This finding has produced an explosion of interest among both experimentalists and theorists. It has been verified repeatedly, although very few of the investigators have given truly quantitative estimates of the enhancement, and it promises to become a useful tool for surface studies.

Despite intense theoretical speculation, the origin of SERS has been puzzling. A proper explanation must contend with a number of factors, namely (1) the very critical sensitivity of the enhancement to the degree of roughening, (2) the fact that heretofore only adsorption on silver, and to a lesser extent upon gold and copper has produced large effects, (3) the manner in which the enhancement falls off with distance of the species from the surface, (4) the depolarization of otherwise strongly polarized bands, (5) the dependence of the enhancement upon the wavelength of the excitation, and (6) specific chemical effects.

The various mechanisms proposed to account for SERS may be classified as either electromagnetic or chemical. Chemical mechanisms ascribe the effect to interactions between metallic electrons and the adsorbate giving rise to electronic states which exhibit strong resonances. Electromagnetic mechanisms consider that the electric field of the light wave is enhanced by its interaction with the roughened metallic surface. In that case, the molecule merely responds to the amplified field.

One of the difficulties in developing a theory is knowing just how to describe a so-called rough surface which is depicted in Fig. 2. A somewhat simpler, if rather naive model, can be envisaged as a layer of colloidal metal spheres covered with adsorbate, atop a smooth metal surface. Yet even this poses great difficulties for theoretical analysis and it was suggested in 1978 by Moskovits in Canada that truly colloidal spheres covered with adsorbate and isolated in a dielectric medium might display similar enhancements. Such a model might be more tractable to theoretical analysis.

Creighton, Blatchford and Albrecht in England followed this suggestion and measured enhancement of pyridine on silver hydrosols as high as 250-fold and although this was not nearly as great as the 10^5 and 10^6 enhancement measured by Van Duyne on roughened silver surfaces, it did suggest that the same effect might be occurring in the colloidal system. I think you can see how this thought process of Moskovits and the experiment by Creighton have transformed this problem in surface science to a problem in colloid science.

As I have already noted, among the explanations proposed to account for SERS was the suggestion that the enhancement was due to the effect of the roughened silver surface upon the electromagnetic radiation. Creighton believed that the effect was electromagnetic and that it was in some way related to the absorption and scattering of light by the silver particles. It was a letter from Creighton in the summer of 1979 that interested me in the problem.

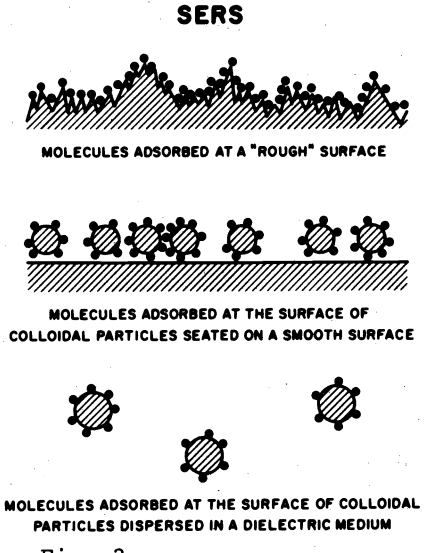

Fig. 2

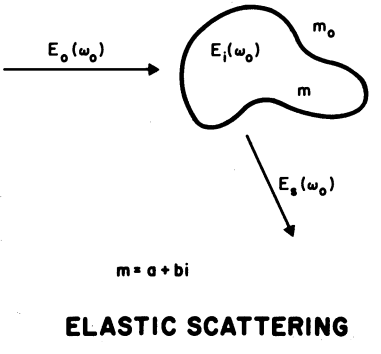

Fig. 3

Since we had been studying the effect of embedment of Raman and fluorescent molecules within colloidal particles, it seemed reasonable to extend our classical electrodynamic model to the case where the inelastically scattering molecules are located outside of the particle and to see whether such an analysis might give rise to enhancements comparable to those which had been observed. We have completed the theory for molecules adsorbed at the surface

of colloidal spheres and have found that it does predict the main features of SERS. Furthermore, by utilizing a colloidal silver sol for which our theory predicts enhancements of the order of 10^6, we have measured Raman signals which are actually enhanced to the same extent.

2. ELASTIC SCATTERING

Let us start our analysis by first considering elastic scattering. By elastic scattering we mean that the scattered radiation has the same wavelength as the irradiating beam. The model is illustrated in Fig. 3. A particle which is characterized by its morphology (meaning its size, shape and orientation) and its refractive index m, is irradiated by a plane electromagnetic wave at some frequency ω_o propagating in a medium of refractive index m_o. The wave penetrates the particle where it is described by the field $\vec{E}_i(\omega_o)$. Outside of the particle the field can be described by the superposition of the incident field $\vec{E}_o(\omega_o)$ plus the so-called scattered field $\vec{E}_s(\omega_o)$. This can be formulated as a boundary value problem whose solution completely characterizes the scattered electromagnetic field as well as the electromagnetic field inside the particle. The scattered radiation, as well as any radiation which may be absorbed within the particle, is a complicated function of particle size, shape and complex refractive index.

3. INELASTIC SCATTERING BY EMBEDDED MOLECULES

We now turn to inelastic scattering, of which fluorescence and the Raman effect are examples. In this case, there is excitation of electronic and vibrational transitions at one wavelength and emission of light at some shifted wavelength. The intensity, polarization and angular distribution of the inelastic signals, as well as their wavelength distribution, are related to the incident radiation through a phenomenological molecular parameter, the polarizability tensor.

There are several important areas of investigation where inelastically scattering molecules are embedded within small particles of which the most active are flow fluorimetry of biological cells and Raman microprobe analysis of colloids. A number of years ago, we raised the following query regarding such experiments: How are inelastic signals affected by embedment of active molecules within small particles? We have been able to show in such cases that, in addition to the polarizability tensor, the signals also depend upon the particle size, shape and orientation, upon the refractive index of the particle and upon the spatial distribution of the active molecules within the particle.

The model is shown in Fig. 4. As we have already seen when discussing elastic scattering, there is an incident field $\vec{E}_o(\omega_o)$ which illuminates the particle, an internal field $\vec{E}_i(\omega_o)$ and a scattered field $\vec{E}_s(\omega_o)$.

We consider that a particular inelastic scattering molecule is located at some position $\vec{r}'$ within the particle. This molecule will be excited by the radiation field at the incident frequency inside the particle and it will emit radiation at the shifted frequency. When this emission is dipolar, the dipole moment is equal to the incident internal field at $\vec{r}'$ multiplied by a polarizability tensor i.e. $\vec{p}(\omega,\vec{r}') = \alpha\vec{E}_i(\omega_o,\vec{r}')$. For a sphere this internal field can be obtained from the same theory elaborated by Gustav Mie for metal hydrosols. As for the polarizability tensor, we will assume that it is the same as in the bulk medium. In other words, the molecule is unable to feel the edge of the particle; it does not know that it is located in a particle and it responds to the radiation as if it were in an extended medium. The radiation on the other hand is very sensitive to the particle morphology and it varies from position to position within the particle.

The electromagnetic field $\vec{E}_i(\omega,\vec{r}',\vec{r}")$ at some position $\vec{r}"$ is due to the emission by the molecule located at $\vec{r}'$. We will arrange that this field be composed of two parts. The first part is the field due to the dipole $\vec{E}_{dip}(\omega_o,\vec{r}',\vec{r}")$ as if that dipole, located at $\vec{r}'$ were embedding in an extended, bulk medium instead of inside a small particle. The second part is an induced field $\vec{E}_{die}(\omega,\vec{r}',\vec{r}")$ which compensates for the effect of the particle boundary. In addition there is the outgoing Raman or fluorescent scattered field $\vec{E}_s(\omega,\vec{r}')$ due to the dipole at $\vec{r}'$. What we have just done is to formulate a new boundary value problem.

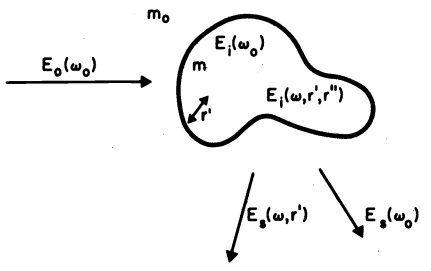

INELASTIC SCATTERING
MOLECULE AT r' EMBEDDED WITHIN PARTICLE

Fig. 4

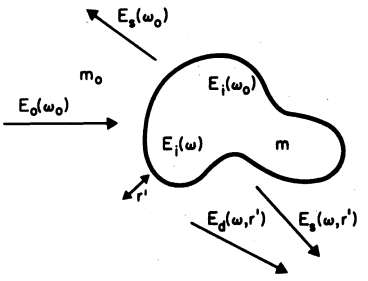

INELASTIC SCATTERING
MOLECULE AT r' OUTSIDE OF PARTICLE

Fig. 5

Since $\vec{E}_S(\omega,\vec{r}')$ is the solution for only a single molecule located at position $\vec{r}'$, it is necessary, finally, to add the results for an array of molecules, uniform or otherwise, corresponding to the particular distribution of material within the particle.

We have, up to now, formulated the theory for spheres, concentric spheres, long cylinders and spheroids and we have carried out numerical calculations to illustrate some of the features. Professor Chang at Yale and Professor Kratohvil at Clarkson have verified some of the main predictions of the theory by experiments with fluorescent polymer latexes.

4. MODEL FOR SERS

We are now ready to discuss surface enhanced Raman scattering. My own interest was piqued by the work of Creighton with silver and gold hydrosols about which I spoke earlier. He had tried to correlate his observation of the dependence of the enhancement upon the wavelength of the excitation radiation with the absorption spectrum of the silver hydrosols upon which the Raman scattering molecules were adsorbed. Indeed, it was a similar interest in the absorption spectrum of colloidal silver and gold by Michael Faraday and the subsequent use of electromagnetic theory by Gustav Mie to investigate that problem that led to the foundation of colloid optics. We shall pursue that clue.

It has been a fairly straightforward path, at least conceptually, from Mie's theory of elastic scattering to our model of inelastic scattering by molecules embedded within small particles about which I have just spoken. We have now extended that model to the case where the Raman scattering molecules are adsorbed at the outer surface of a colloidal particle. Our theory predicts, under appropriate conditions, an enhancement of 10^6 for Raman scattering molecules adsorbed at the surface of colloidal silver. Accordingly, classical electromagnetic theory can account for surface enhanced Raman scattering. Furthermore, we have recently measured Raman signals from citrate adsorbed at the surface of colloidal silver particles and we have found that these are enhanced by as much as a factor of 6×10^5. Thus, theory and experiment, at least for colloidal particles, are in accord. I will now describe the theory and then tell you about the experiments.

The model is depicted in Fig. 5. The molecule, which is presumed to behave as a classical oscillating dipole, is located at position $\vec{r}'$ outside of an isotropic, homogeneous sphere, including positions on the surface. There are no restrictions on the particle radius or the refractive index. The electric field outside the particle at frequency ω_o, is comprised of the field of the incident plane electromagnetic wave $\vec{E}_o(\omega_o,\vec{r})$ and the scattered field $\vec{E}_S(\omega_o,\vec{r})$ which is obtained from Mie's theory. This field at the position of the dipole excites the dipole to radiate at the Raman frequency with dipole moment $\vec{p}(\omega,\vec{r}') = \alpha[\vec{E}_o(\omega_o,\vec{r}') + \vec{E}_S(\omega_o,\vec{r}')]$ where α is the Raman

polarizability tensor. The Raman radiation from the dipole at $\vec{r}'$ at the observer position is given by $\vec{E}_R(\omega,\vec{r}') = \vec{E}_d(\omega,\vec{r}') + \vec{E}_s(\omega,\vec{r}')$. The field that the dipole would radiate if the particle were absent is given by $\vec{E}_d(\omega,\vec{r}')$ whereas $\vec{E}_s(\omega,\vec{r}')$ is an additional contribution due to scattering of the dipole field by the particle.

Once again we have formulated a new boundary value problem which we have solved for a spherical particle. We are hopeful that it will also be possible to obtain solutions for long cylinders and for spheroids. Just as for molecules distributed within the particle, the result for a distribution of molecules outside of the particle or at the surface of the particle is obtained by appropriate superposition of the single molecule results. Such superposition can be obtained either for incoherent or coherent emission. Also, it is necessary in addition to the polarizability tensor, to specify the orientation of the dipole with respect to the particle surface. The solution contains complete information about the amplitude, phase and polarization at any positions outside of a spherical particle of any size or optical constants.

5. SERS—NUMERICAL RESULTS

I will now present only one set of numerical results which pertain to SERS of the 1010 cm^{-1} band of pyridine adsorbed on a silver hydrosol. This will illustrate a crucial feature of SERS. Figure 6 shows the enhancement as a function of excitation wavelength for three particle radii, 5, 50 and 500 nm. These calculations are for a single dipole at a particular location, on the particle surface for an observer also at a particular location. Although the results for a monolayer and for other observer locations vary somewhat, the main qualitative features are the same as for this more rapidly calculable result. The calculated enhancement is the ratio of the signal that would be observed from a molecule oriented perpendicular to the surface compared with a randomly oriented molecule in solution having the same polarizability tensor.

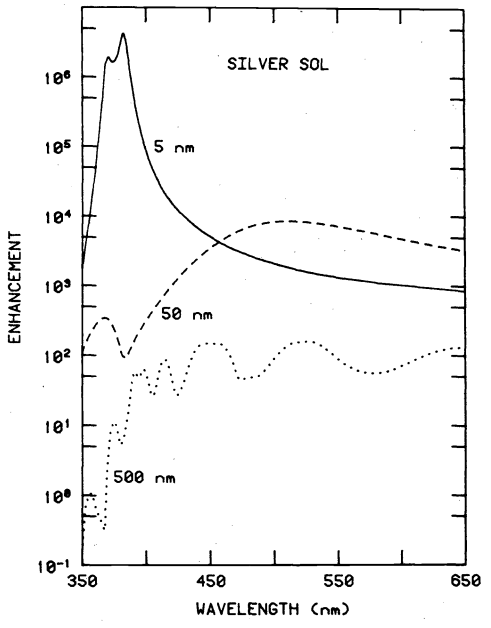

Fig. 6. Enhancement vs. excitation wavelength for silver spheres in water with radii 5, 50, 500 nm.

The smallest particle exhibits a sharp peak somewhat greater than 10^6 at 382 nm which drops off rapidly at both higher and lower wavelengths. Yet even these lesser values are greater than 10^3. For the 50 nm particle the enhancement peak of nearly 10^4 is much broader and it is shifted to a longer wavelength. For the still larger 500 nm particle the very much smaller enhancement oscillates in the range 10 to 10^2 throughout the visible and then decreases to values of less than unity in the ultraviolet.

I will only take time to discuss the origin of the very sharp peak at 382 nm for the 5 nm particle because it will provide some insight into the physical process. Because this particle size is small compared to the wavelength it is possible to derive a simple limiting expression for the enhancement G_{v_v}

in Table 1 in which m_o is the refractive index of the particle at the incident wavelength and m is the value at the Raman wavelength. The condition for the enhancement to become very large is that either g_o or g becomes very large. This occurs for silver in water at about 382 nm where the refractive index is nearly a purely imaginary number with value $\sqrt{2}i$. Then (m^2+2) becomes close to zero. Actually g never goes to infinity because as (m^2+2) approaches zero the more accurate expression at the bottom of the table must be utilized.

TABLE 1. SERS—SMALL PARTICLE LIMIT

$$G_{V_v} = |1 + 2g_o + 2g + 4gg_o|^2$$

$$g_o = \frac{m_o^2-1}{m_o^2+2} \qquad g = \frac{m^2-1}{m^2+2}$$

Dominant term $\sim|g_o g|^2$

as $m \to \sqrt{2}i$; $(m^2+2) \to 0$

$$g = \frac{(m_o^2-1) - [(k_o a)^2/10](m_o^4-1)}{(m_o^2+2) - [(k_o a)^2/10](10-9m_o^2-m_o^4)}$$

The origin of the enhancement is now clear. It occurs at a particular resonance condition where the free electrons in the metal oscillate in phase with the oscillating electromagnetic field. For a bounded body, there are characteristic modes comprised of oscillating standing waves. Each mode is set into resonance at a characteristic frequency. For a small particle the electric dipole mode, called the dipolar surface plasmon, dominates and this is set into resonance at the frequency for which $m = \sqrt{2}i$. According to this model, SERS arises because of the enhancement of the electromagnetic field by resonance of the electrons in the particle. The effect is particularly large because of the coupling of the process at both the incident and the Raman wavelengths. It is particle size dependent as we have already seen and it also depends upon the manner in which the complex refractive index varies with wavelength. It is evident that the very large enhancement peak occurs when the particles are small and the wavelength corresponds to a refractive index for which there is an optical resonance.

6. SERS—EXPERIMENTS

I will now proceed to describe briefly some preliminary experimental results. A dense red silver hydrosol, prepared by Carey Lea's method, was comprised of 21 nm average radius particles as estimated by comparison of the measured absorbance with calculated values. The particles have been shown to be covered by a monolayer of citrate, each ion occupying an area of $38A^2$. By assuming that all of the silver introduced as $AgNO_3$ is retained throughout the preparative procedure and converted to colloidal silver we were able to calculate a concentration of 6.4×10^{-6}M adsorbed citrate in our samples. This is an overestimate which results in underestimation of the enhancement.

Raman spectra of these sols were measured at five wavelengths. Measurements were also made under identical conditions of 1.37 M sodium citrate. The measured Raman signals arose from the adsorbed citrate since the supernatant of the sols did not show any detectable Raman bands.

The strong dependence of the enhancement upon the incident wavelength is illustrated in Fig. 7 where the bands at 1400 cm^{-1} from the 1.37 M citrate on the left are compared with those from the sols on the right. The excitation

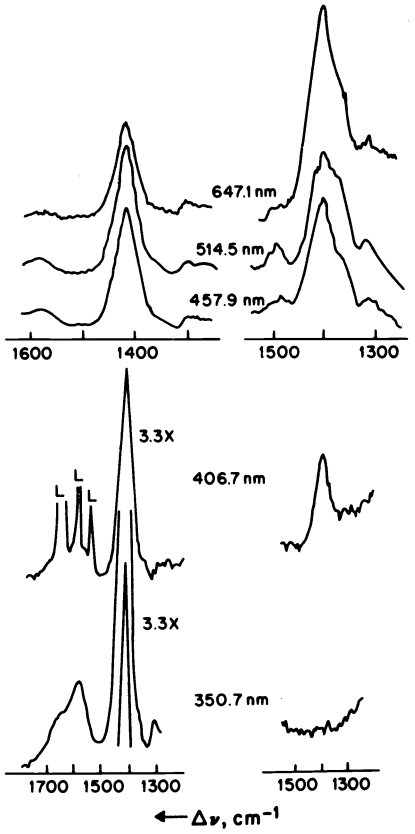

Fig. 7. Raman bands for excitation at λ_o = 350.7, 406.7, 457.9, 514.5 and 647.1 nm. Left hand side 1.37 M sodium citrate. Right hand side, Carey-Lea sol.

wavelengths, proceeding up the figure are 350.7, 406.7, 457.9, 514.5, and 647.1. Numerical values of the enhancement are obtained by multiplying the ratio of the area under the sol Raman band to that under the sodium citrate band by the ratio of the sodium citrate concentration (1.37 M) to the sol concentration (6.4×10^{-6}). The enhancements which are listed in Table 2 vary from less than 3×10^{3} in the ultraviolet to 6.0×10^{5} in the red. We believe that these numerical values are among the most accurate which have been measured.

TABLE 2. MEASURED AND CALCULATED RAMAN ENHANCEMENTS

Wavelength (nm)	Integrated band intensity relative to 1.37 M Na citrate	Measured enhancement	Calculated enhancement for various radii (nm)	
			20	50
350.7	<0.014	$<3.1\times10^{3}$	3.4×10^{2}	5.4×10^{1}
406.7	0.14	3.1×10^{4}	5.2×10^{4}	5.6×10^{2}
457.9	1.5	3.2×10^{5}	1.7×10^{3}	1.2×10^{3}
514.5	1.7	3.6×10^{5}	5.6×10^{2}	1.7×10^{3}
647.1	2.8	6.0×10^{5}	2.1×10^{2}	6.0×10^{2}

Also listed in the table are values of the enhancements for the 1400 cm^{-1} band, calculated for various particle sizes by using our theoretical model. Both theory and experiment give maximum enhancements of nearly 10^{6}; however, the wavelength dependences differ. Whereas the theoretical curve for a 20 nm radius particle shows a sharp peak near 400 nm with a sharp drop-off at both higher and lower wavelengths, the measured enhancements do not display this peak but appear to increase monotonically with increasing wavelength.

7. SERS FOR SPHEROIDS

This discrepancy between the measured dependence of the enhancement upon excitation wavelength and the dependence predicted by theory has been of concern but we now believe we have resolved it. The clue is that the resonance condition in which SERS has its origin changes if the system varies from an isolated sphere to isolated particles of other geometries or to a collection of interacting particles. For small spheres (i.e., small compared to the wavelength) the resonance condition occurs whenever the denominator of the expression $(m^2-1)/(m^2+2)$ in Table 1 becomes small, i.e., whenever the refractive index approaches the values of the purely imaginary number $\sqrt{2}i$. For a small ellipsoid of revolution—a spheroid—there are two resonance conditions and these depend not only on the refractive index but also on the shape of the spheroid. Indeed, the resonance condition is very sensitive to shape. Accordingly, for a dispersion comprised of a distribution of particle morphologies the dependence of the net Raman enhancement upon wavelength will be determined by an appropriate distribution of resonant frequencies.

Figure 8 depicts the calculated enhancement of the 1010 cm^{-1} Raman band over the excitation wavelength range 350 to 650 nm for randomly oriented monolayer-covered silver prolate spheroids with axial ratios equal to 1.0, 1.5, 2.0, 2.5 and 3.0. The maximum enhancement increases in magnitude and shifts toward longer excitation wavelengths as the axial ratio increases. Accordingly, virtually any excitation profile can be constructed by superposition of signals from an appropriate distribution of shapes.

An interesting aspect of each excitation curve is the two closely spaced peaks which are always separated precisely by the Raman shift, in this case 1010 cm^{-1}. Still another interesting aspect is that the second of each pair of peaks (the peak occurring at the longer wavelength for a Stokes shift) always occurs at the same excitation wavelength no matter what the magnitude of the Raman shift.

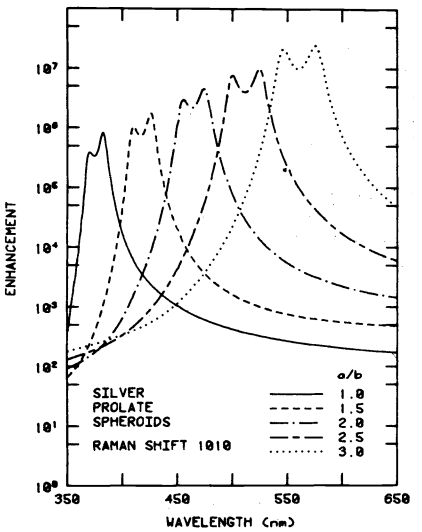

Fig. 8. Enhancement vs. wavelength for silver prolate spheroids.

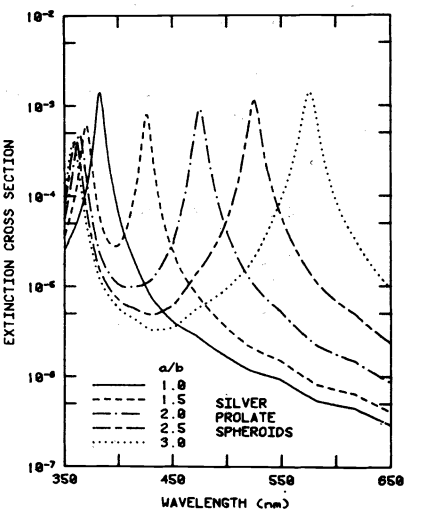

Fig. 9. Extinction vs. wavelength for silver prolate spheroids.

The origin of this dual peak structure can be understood if we consider the extinction cross sections for randomly oriented silver spheroids shown in Fig. 9 over the same range of wavelengths and the same axial ratios as for the Raman curves in Fig. 8. The extinction cross section, which is related to the transmittance, is the sum of the scattering and absorption cross sections. The central features of these curves are the two sharp extinction peaks for the spheroids and the single peak for the sphere. The two extinction peaks correspond to the two resonance conditions which were referred to earlier.

Comparison of this figure with the previous one will show that the second of the dual Raman peaks is located at the same excitation wavelength as the wavelength for the major extinction maximum. Figure 10 illustrates the

physical origin of the double peak. Let us recall that in the present model the Raman field is the product of two processes, viz. (1) stimulation of the molecule by the local field at the incident wavelength, (2) scattering by the particle of the Raman field at the shifted wavelength. Accordingly, the second of each pair of peaks, being at the same wavelength as the peak in the extinction curve, is due to stimulation of the Raman process by the strong local field at the incident wavelength. This field corresponds to the condition for resonance of the dipolar surface plasmon. On the other hand at the wavelength of the first Raman peak, stimulation is by an incident wavelength which is somewhat off resonance but now the Raman shifted signal is enhanced because it interacts (scatters) with the particle at the resonance condition. The resolution of discrete peaks at these two wavelengths requires that the extinction peak itself be sufficiently sharp.

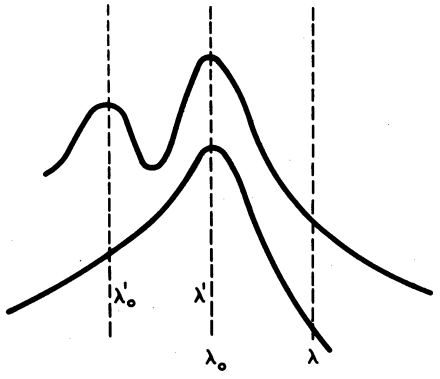

Fig. 10. Schematic representation of enhancement (upper curve) and extinction (lower curve) vs. wavelength. λ_o represents incident wavelength tuned into extinction peak. λ'_o represents incident wavelength such that Raman wavelength λ' is tuned into extinction peak.

Similar calculations for gold prolate spheroids are shown in Fig. 11. For gold, reported measurements as well as our earlier calculations have given enhancements about two to three orders of magnitude less than those for silver. However, the sensitivity of the enhancement to the particle eccentricity is quite striking. Not only does the maximum shift to longer excitation wavelength as for silver, but in this case the enhancement increases sharply from $\sim 10^3$ to $\sim 2\times10^6$ as the axial ratio increases from 1.0 to 3.0. The extinction curves for gold, shown in Fig. 12, exhibit a corresponding pattern. The extinction maxima increases about an order of magnitude as the particle is extended from a sphere to a prolate spheroid with an axial ratio of 3.0.

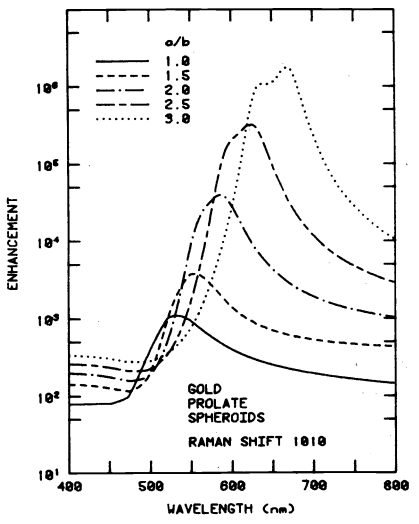

Fig. 11. Enhancement vs. wavelength for gold prolate spheroids.

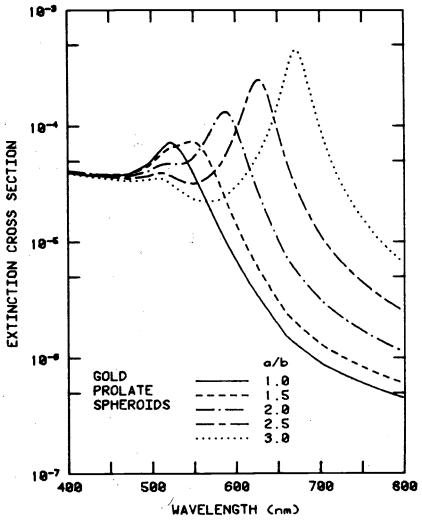

Fig. 12. Extinction vs. wavelength for gold prolate spheroids.

Another aspect is that only the most eccentric spheroid shows a double peak. This is because of the broader extinction curves. Excitation into the extinction peak or Raman scattering into this peak does not result in a significantly greater Raman enhancement than when either of these processes occurs at neighboring wavelengths. The emergence of the double peak for axial ratio 3.0 results from the narrowing of the extinction curve with increasing axial ratio.

We conclude this discussion on spheroids with a warning that the direct correspondence between the peaks in the enhancement and extinction curves only occurs for particles which are small compared to the wavelength. For larger particles these effects are not linked in such a simple linear fashion.

8. CONCLUSION

It is now clear that the electrodynamic model of SERS is quite capable of accounting for a wide range of qualitative and quantitative features of this phenomenon. We have omitted from this present discussion any consideration of the orientation of the molecular dipole at the surface or the distance of the dipole from the surface as well as the effect of the various physical parameters upon the angular distribution and polarization of the Raman scattered radiation. Still remaining for theoretical analysis are dipole-dipole interaction which should depend upon surface coverage, extension of the theory to spheroids and cylinders of arbitrary size and, what we expect to be a most interesting aspect, dielectric particles of various shapes which have been coated with a thin metal film. In the latter case the Raman active molecules may be located either at or near the outer or inner metal surfaces.

Our theoretical approach has been purely physical in that we have assumed that the molecular polarizability of the adsorbed molecule is the same as that of the molecule in the gaseous or liquid medium. Of course that cannot be the case. However, the theory accepts the molecular Raman polarizability as input. If the polarizability of the molecule adsorbed at a smooth macroscopic surface can be ascertained experimentally or by theoretical analysis, its value can be inserted into the formalism. This would then combine what we referred to at the outset as the electromagnetic and chemical mechanisms.

There is a final aspect which has not yet been mentioned, namely, that this analysis suggests that there be comparable enhancements of fluorescence. In addition to our experimental work mentioned earlier for molecules embedded in latex spheres, there have been reports of fluorescent enhancement for dye-coated silver island films. We have proposed, in view of the possibility of both surface enhanced Raman and surface enhanced fluorescent scattering that the acronym SERS might accordingly be changed to SERFS despite the loss of station that this might imply.

Perhaps the most important point to note at this time is that these large Raman band enhancements of species adsorbed at the surface of silver colloids permit structural, kinetic and analytical studies similar to those at roughened electrode surfaces. It is my perception that colloidal hydrosols, as a substrate, have a number of advantages over roughened macroscopic surfaces. These include (1) ease of formation and manipulation, (2) ability to control and vary particle size and shape, (3) more easily definable surface area, (4) a more direct calculation of the enhancement value and (5) a more tractable morphology for theoretical analysis. We are now embarking upon a comprehensive experimental program in the hope that this conjunction of a most classical area of colloid science with this new discovery in surface science may prove fruitful.

9. ACKNOWLEDGMENTS

My collaborators in the SERS work have been Professors Dau-Sing Wang, Herman Chew and Olavi Siiman and Mr. Lloyd Bumm. This work has been supported by NSF Grant CHE-8011444 and ARO Grant DAAG29-79-C-0059.

10. BIBLIOGRAPHY

Numerous references to the work of others is contained in the following papers of our work where further details of the theory and experiments discussed here may be found.

1. D.S. Wang, H. Chew, and M. Kerker, Appl. Opt. 19, 2256-7 (1980).
2. M. Kerker, D.S. Wang, and H. Chew, Appl. Opt. 19, 4159-4174 (1980).
3. M. Kerker, O. Siiman, L.A. Bumm, and D.S. Wang, Appl. Opt. 19, 3253-3255 (1980).
4. D.S. Wang and M. Kerker, Phys. Rev. IN PRESS.